

A simple and effective method for determination of the antithyroid drug carbimazole using ruthenium trichloride

Mukul SHARMA¹, Afraim KOTY², Abdul Jabbar AL-RAJAB^{1,*}

¹Center for Environmental Research & Studies, Jazan University, Jazan, Saudi Arabia

²Department of Chemistry, College of Sciences for Girls, Jazan University, Jazan, Saudi Arabia

Received: 16.01.2017

Accepted/Published Online: 12.07.2017

Final Version: 20.12.2017

Abstract: An accurate, precise, and simple spectrophotometric method is proposed for the determination of the antithyroid drug carbimazole using ruthenium(III) chloride. This method is based on the formation at room temperature of a stable yellow-colored complex with λ_{max} 370 nm. The method has a Beer's law range of 7.81 to $1.95 \times 10^2 \mu\text{g mL}^{-1}$, molar absorptivity coefficient $\epsilon = 1.519 \times 10^3 \text{ L mol}^{-1} \text{ cm}^{-1}$, and correlation coefficient of 0.997. The metal:ligand (M:L) ratio of the complex was confirmed by the mole ratio and Job's method of continuous variation, suggesting a 1:2 stoichiometry. The formed carbimazole:Ru(III) complex was confirmed by spectral studies, including Fourier transform infrared, nuclear magnetic resonance, electron spin resonance, magnetic susceptibility, thermal analysis, and powder-X-ray diffraction. Our method could be adopted for routine analysis of carbimazole, due to its ease, affordability, and effectiveness.

Key words: Carbimazole, pharmaceutical, detection, Ru(III), Fourier transform infrared, spectrophotometric

1. Introduction

Carbimazole (CBZ) (Figure 1), ethyl 3-methyl-2-thioxo-4-imidazoline-1-carboxylate, is used to treat hyperthyroidism by reducing the intake of iodine. It also reduces the formation of diiodotyrosine and hence thyroxine. Carbimazole, upon absorption into the body, is converted into its active form, methimazole, which prevents the coupling of the thyroid peroxidase enzyme and iodination of the tyrosine residues on thyroglobulin,¹ thereby reducing the production of the thyroid hormones T3 and T4 (thyroxine).

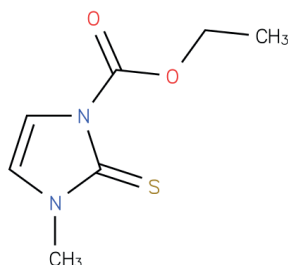


Figure 1. Structure of carbimazole.

Thyroid disease has become a serious public health problem in several countries; therefore, detection of its drugs has become a prime clinical consideration. For this reason, several analytical procedures have

*Correspondence: alrajab@hotmail.com

been developed for the determination of carbimazole. These methods include a colorimetric method using dichromate and molybdate for the assay of carbimazole in drug formulations;² bromometric determination using N-bromosuccinimide and methyl red as an indicator;³ a spectrophotometric method utilizing potassium dichromate, sulfuric acid, and heating at 90 °C for 25 min;⁴ and determination of carbimazole in tablet form with iodine azide.⁵ Apart from these routine analyses, several tedious methods have also been reported, including the determination of carbimazole by first and third derivative spectrophotometry;⁶ a flow-injection method using Pd(II) with λ_{max} of 325 nm;⁷ a flow-injection with chemiluminescence detection of carbimazole in pharmaceutical samples;⁸ a spectrophotometric and spectrodensitometric method based on the reaction with potassium bromate in bromide solution having λ_{max} of 517 nm; and densitometric evaluation of thin-layer chromatograms of carbimazole at 291 nm.⁹ Hydrolysis of carbimazole was studied by polarography and spectrophotometry.¹⁰ Carbimazole was studied by voltammetry and polarography on a mercury electrode.¹¹ A reversed phase HPLC method was developed for carbimazole determination in bulk drugs and formulations.¹² Fourier transform infrared (FTIR), FT-Raman, and UV-Vis techniques and quantum chemical calculation of carbimazole have also been reported.¹³

This literature survey indicates that not much work has been done regarding the possible determination of carbimazole using metals. We were therefore prompted to investigate the use of metals, such as ruthenium, which provide a wide range of oxidation states and are relatively nontoxic.^{14,15} Spectrophotometry is an effective and widely used technique, so a combination of both spectrophotometry and metal complexation could result in an easy and simple determination method for carbimazole in tablet form.

2. Results and discussion

2.1. Optimization of the reaction conditions

Figures 2a and 2b show the UV-visible spectrum of carbimazole and its Ru(III) complex. Good results were achieved by optimizing the reaction conditions by varying the temperature, pH, and time. The effect of temperature was studied by maintaining the temperature range from 25 °C to 80 °C with a thermostat. An increase in temperature decreased the absorbance and color intensity (Figure 3), so room temperature (25 °C) was considered appropriate for maximum color intensity; all subsequent experiments were carried out at 25 °C (± 5 °C).

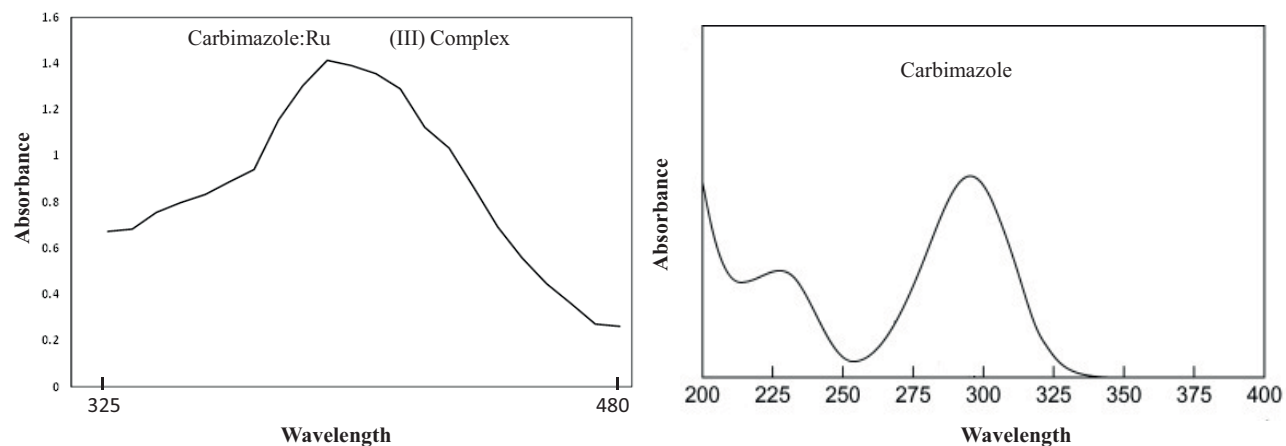


Figure 2. a, b) UV-Vis spectrum of carbimazole and its Ru(III) complex.

The effect of pH was tested to determine whether the color intensity or absorbance of the formed carbimazole:Ru(III) complex would decrease in response to pH changes. Hydrochloric acid was used to acidify the solution (pH 3–4) and sodium hydroxide was used to raise the pH (pH 9–10).

The time required for complexation was studied by measuring the absorbance of a sample solution against a blank solution at different time intervals from 5 to 60 min (Figure 4). The time required for the complexation was 20 min at λ_{max} of 370 nm. No extreme change in the color intensity was observed even after 12 h.

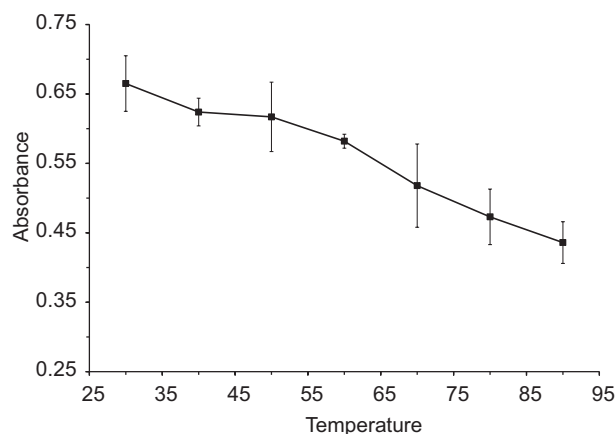


Figure 3. Effect of temperature ($^{\circ}\text{C}$) on the absorbance of the carbimazole:Ru(III) complex.

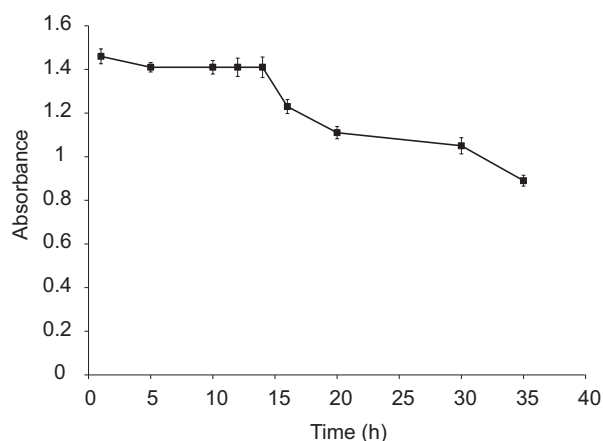


Figure 4. The time course for complexation.

2.2. Stoichiometry

The stoichiometry of the complex was studied by Job's method of continuous variation according to Ragehy et al.¹⁶ (Figure 5) and the mole ratio method (Figure 6).

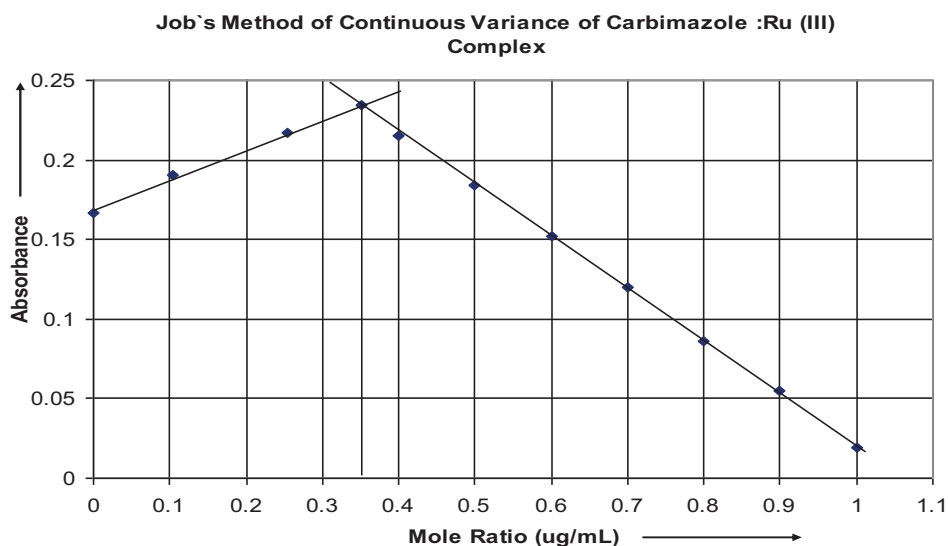


Figure 5. Job's method of continuous variation.

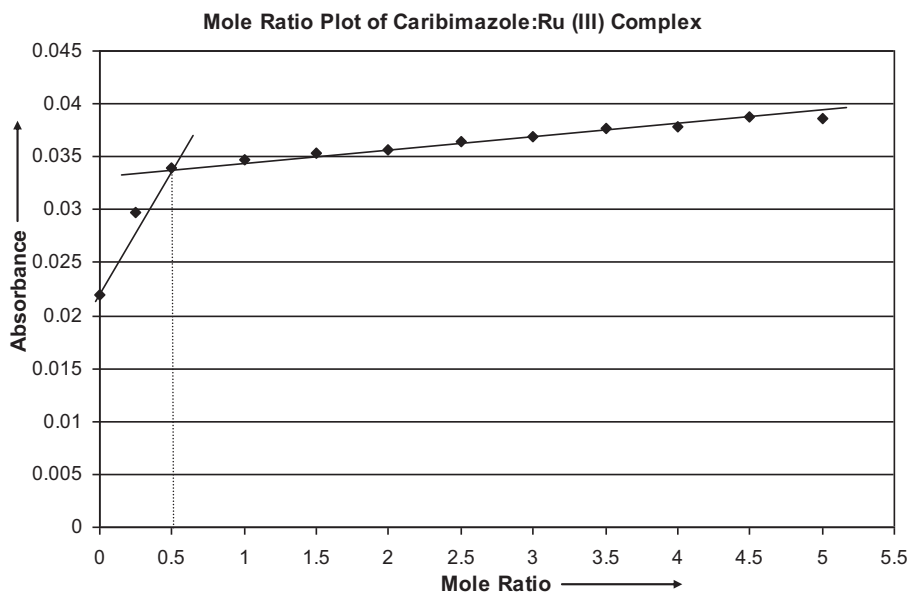


Figure 6. Mole ratio graph of carbimazole:Ru(III) complex.

Job's method was conducted by preparing a series of solutions with a constant total volume of metal ion Ru(III) and ligand (drug carbimazole). Here, the sum of the total analytical concentration of the complexing agent (drug carbimazole) C_x and metal ion Ru(III) C_m was held constant and only their ratios were varied.

The absorbance of each solution mixture was measured at the λ_{max} of the complex (370 nm). The absorbance and mole fraction of the ligand C_x/C were then presented graphically. The sides of the curve were extrapolated to their point of intersection (n). Composition of the Ru(III):carbimazole complex was then calculated as 1:2 as follows.

$$n = C_x/C_m = x/1 - x$$

$$= 0.34/1 - 0.34$$

$$C_x/C_m = 0.5 = 1/2$$

$$2C_x = C_m$$

$$M : L = 1 : 2$$

By contrast, the mole ratio method was conducted by preparing a series of solutions in which the concentration of one reactant [metal ion Ru(III)] was kept constant and the concentration of the other (the carbimazole ligand) was varied. The absorbance of each solution was measured at 370 nm.

A graph drawn between absorbance and the mole ratio of the reagent gives a straight line with a positive slope from the origin up to mole ratio value two and then becomes horizontal. This shows that the metal has been consumed completely at a mole ratio of two and that further addition of ligand produces no additional complexation. Thus, the composition of the complex was 1:2 for the Ru(III):carbimazole complex as determined by the mole ratio method.

2.3. Stability constant of the complex

The stability formation constant (K_f) of the carbimazole:Ru(III) complex was evaluated according to a previous study.¹⁷ The color intensity and absorbance were constant for a maximum of 12 h. The stability constant can be calculated from the following equation:

$$K_f = \frac{\frac{A}{A_m}}{\left\{ \frac{(1-A)}{A_m} \right\}^{n-1}} C^n n^n$$

where A and A_m are the absorbance and maximum absorbance obtained from Job's method, n is the ratio of carbimazole:Ru(III), C is the molar concentration of carbimazole, and K_f is the stability formation constant, which was determined as 2.1 for the carbimazole:Ru(III) complex.

2.4. Analytical parameters

The linearity of the complex formation was evaluated using Beer's law and the graph of concentration versus absorbance (Figure 7), which indicated a good linearity range from 7.81 to $1.95 \times 10^2 \mu\text{g mL}^{-1}$, with molar absorptivity (ϵ) = $1.519 \times 10^3 \text{ L mol}^{-1} \text{ cm}^{-1}$. The linear regression equation for the carbimazole:Ru(III) complex was determined as follows (Table 1):

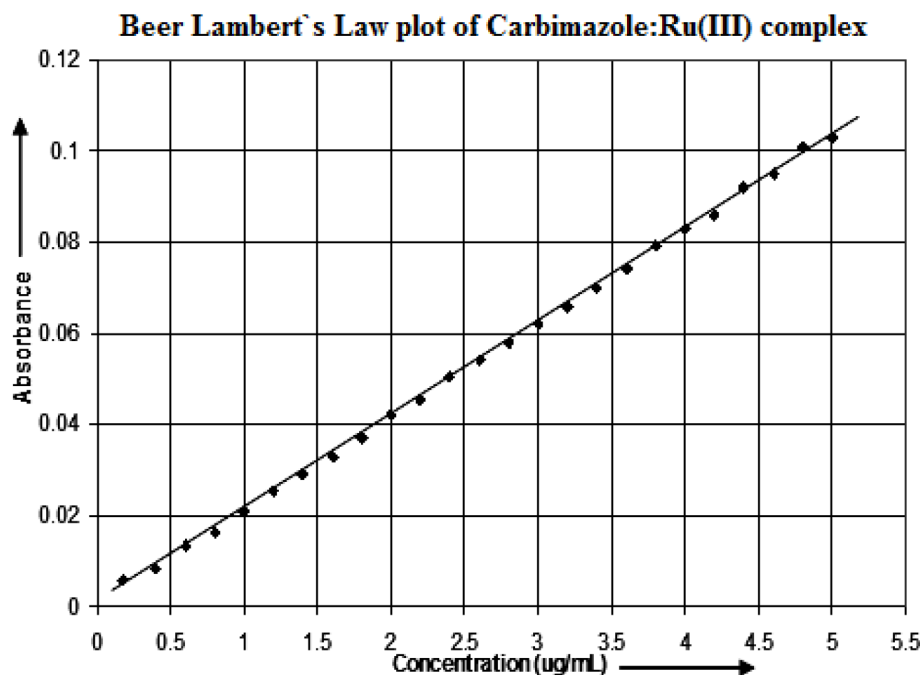


Figure 7. Beer-Lambert law plot for the carbimazole:Ru(III) complex.

$$Y = 6.01 \times 10^{-3} + 1.09 \times 10^{-2} X$$

The correlation coefficient r was 0.99, slope $b = 1.09 \times 10^{-2}$, and intercept $a = 6.031 \times 10^{-3}$. The relative standard deviation (RSD) was 1.89, LOD and LOQ were respectively found to be $1.83 \mu\text{g mL}^{-1}$ and $5.53 \mu\text{g mL}^{-1}$, and the standard analytical error was 0.763 for the carbimazole:Ru(III) complex. The present method was compared with the reported methods (Table 2) and was found to be more accurate and precise.

Table 1. Microdetermination of carbimazole as its Ru(III) complex.

S. no.	Weight taken (in μg)	Weight found (in μg)	Standard deviation	Coefficient of variation	Regression Eq.* statistical data
1	7.81	8.98	3.88×10^{-02}	4.29×10^{-01}	LOD = 1.83 $\mu\text{g mL}^{-1}$ Slope $b = 1.09 \times 10^{-2}$ LOQ = 5.53 $\mu\text{g mL}^{-1}$ Intercept $a = 6.031 \times 10^{-3}$ Correlation coefficient $r = 0.99$
2	$1.56 \times 10^{+01}$	$1.70 \times 10^{+01}$	2.78×10^{-02}	1.69×10^{-01}	
3	$2.34 \times 10^{+01}$	$2.42 \times 10^{+01}$	2.92×10^{-02}	1.20×10^{-01}	
4	$3.12 \times 10^{+01}$	$3.22 \times 10^{+01}$	3.38×10^{-02}	1.05×10^{-01}	
5	$3.91 \times 10^{+01}$	$4.06 \times 10^{+01}$	5.45×10^{-02}	1.36×10^{-01}	
6	$4.69 \times 10^{+01}$	$4.75 \times 10^{+01}$	1.28×10^{-02}	2.68×10^{-02}	
7	$5.47 \times 10^{+01}$	$5.59 \times 10^{+01}$	2.30×10^{-02}	4.11×10^{-02}	
8	$6.25 \times 10^{+01}$	$6.33 \times 10^{+01}$	1.10×10^{-02}	1.74×10^{-02}	
9	$7.03 \times 10^{+01}$	$7.09 \times 10^{+01}$	2.55×10^{-02}	3.57×10^{-02}	
10	$7.81 \times 10^{+01}$	$7.99 \times 10^{+01}$	1.91×10^{-02}	2.40×10^{-02}	
11	$8.59 \times 10^{+01}$	$8.71 \times 10^{+01}$	2.30×10^{-02}	2.64×10^{-02}	
12	$9.37 \times 10^{+01}$	$9.51 \times 10^{+01}$	1.69×10^{-02}	1.77×10^{-02}	
13	$1.02 \times 10^{+02}$	$1.02 \times 10^{+02}$	3.31×10^{-02}	3.24×10^{-02}	
14	$1.09 \times 10^{+02}$	$1.11 \times 10^{+02}$	1.10×10^{-02}	9.96×10^{-03}	
15	$1.17 \times 10^{+02}$	$1.18 \times 10^{+02}$	4.18×10^{-02}	3.54×10^{-02}	
16	$1.25 \times 10^{+02}$	$1.26 \times 10^{+02}$	6.38×10^{-03}	5.07×10^{-03}	
17	$1.33 \times 10^{+02}$	$1.35 \times 10^{+02}$	5.74×10^{-02}	4.28×10^{-02}	
18	$1.41 \times 10^{+02}$	$1.41 \times 10^{+02}$	2.21×10^{-02}	1.56×10^{-02}	
19	$1.48 \times 10^{+02}$	$1.50 \times 10^{+02}$	2.55×10^{-02}	1.70×10^{-02}	
20	$1.56 \times 10^{+02}$	$1.57 \times 10^{+02}$	1.69×10^{-02}	1.07×10^{-02}	
21	$1.64 \times 10^{+02}$	$1.64 \times 10^{+02}$	4.46×10^{-02}	2.70×10^{-02}	
22	$1.72 \times 10^{+02}$	$1.73 \times 10^{+02}$	2.92×10^{-02}	1.69×10^{-02}	
23	$1.80 \times 10^{+02}$	$1.81 \times 10^{+02}$	3.19×10^{-02}	1.77×10^{-02}	
24	$1.87 \times 10^{+02}$	$1.89 \times 10^{+02}$	6.38×10^{-03}	3.38×10^{-03}	
25	$1.95 \times 10^{+02}$	$2.05 \times 10^{+02}$	2.30×10^{-01}	1.11×10^{-01}	

*Summation of five determinations.

2.5. Spectral study of the carbimazole:Ru(III) complex

2.5.1. FTIR study

The FTIR spectra were recorded in the range of 4000–400 cm^{-1} using a 1:3 ratio of KBr powder. The spectrum of carbimazole shows a sharp band at 1203 cm^{-1} (Figure 8a), which is assigned to the presence of the C=S group. This group is missing in the complex spectrum, thereby affirming the involvement of the thione group

Table 2. Comparison of present work with reported methods.

	Reagent used	Linear range ($\mu\text{g mL}^{-1}$)	LOD	Application	Reference
Carbimazole	Iodine-azide (TLC and HPTLC)	20–200 μL	0.08 nmol for TLC and 0.04 nmol for HPTLC	Tablets	5
	Pd(II) catalyzed with neutral red and hypophosphite ion	0.04–0.3 ppm	0.02 ppm	Pure and tablets	26
	Cu(II)-catalyzed chemiluminescence (CL) reaction	3–120 mg L^{-1}	-	Tablets	8
	Palladium(II)-catalyzed reaction between the pyronine G and hypophosphite ions (kinetic determination)	0.04–0.70 $\mu\text{g mL}^{-1}$	-	Pharmaceuticals, animal feed, and animal livers	27
	Ru(III) (spectrophotometer)	0.02–1.78 $\mu\text{g mL}^{-1}$	1.83	Tablets	Present method

with the Ru(III) ion. The FTIR spectrum of carbimazole also shows a band at 1699 cm^{-1} associated with the thioimidazole ring. The decrease and alteration of this band to 1658 cm^{-1} in the carbimazole:Ru(III) complex (Figure 8b) indicates the involvement of ring N in the bonding with the Ru(III) ion.

Two sharp bands appear at 1428 cm^{-1} and 1312 cm^{-1} in the carbimazole spectrum,¹⁸ associated with the presence of C=O-O-C stretching. These two bands are very much reduced in the spectrum of the complex, indicating the degradation of the ester group attached to the fifth N atom.

Bands at 929 cm^{-1} and 801 cm^{-1} are attributed to the C-H band (oop)¹⁹ mode of the aromatic ring, which is reduced to 917 cm^{-1} and 872 cm^{-1} in the carbimazole:Ru(III) complex, suggesting high strain due to participation of sulfur and nitrogen groups in binding. A wide array at 3414 cm^{-1} is allocated to OH strain for the lattice water,²⁰ which affirms the existence of H_2O linked with the metal (M) ion through a dative bond. An intermediate band at 460 cm^{-1} associated with Ru-N strain is frequently found in Ru-xyleneol.²¹ The strength of the M-N bond suggests an electrostatic nature; if this bond has a lower frequency, then it features ionic behaviour.²² Similarly, an average sized band at 420 cm^{-1} is assigned to the Ru-sulfur region.

2.5.2. ^1H NMR study

The ^1H NMR spectra were recorded using D_2O CDCl_3 as a solvent and tetramethylsilane (TMS) as an internal standard. The ^1H NMR spectrum of carbimazole (Figure 9a) shows a sharp signal triplet at 1.2 ppm, affirming the CH_3 group of ethyl acetate. This peak completely disappears in the ^1H NMR spectrum of the complex, indicating the elimination of the ethyl acetate group in acidic medium in the complex.

A sharp and high intensity quartet at 4.30 ppm in the carbimazole spectrum is attributed to the CH_2 group of ethyl acetate. This peak completely disappears in the spectrum of the complex, confirming the removal

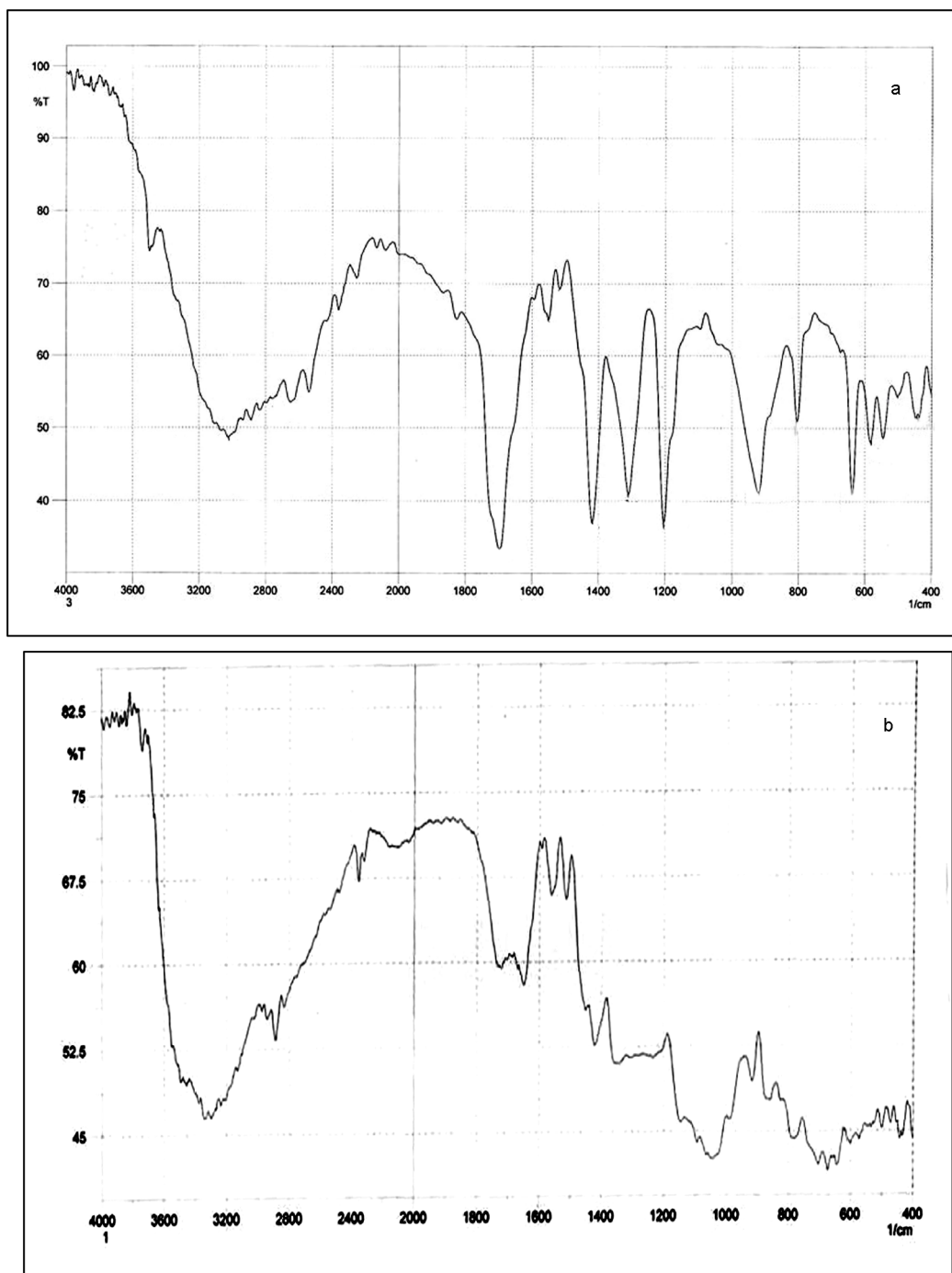


Figure 8. a, b) FTIR spectrum of carbimazole and its Ru(III) complex.

of ethyl acetate from carbimazole in an acidic medium and leaving behind the N-ring, which can easily bind Ru(III) ions. The removal of the ethyl acetate group can also be confirmed by ^{13}C NMR, but the ^1H NMR result is more accurate in the case of carbimazole as it gives clear information about hydrogen removal and the effect of the other H atom.

The $\text{HC}=\text{CH}$ group of the imidazole ring is assigned at 7.38 and 6.8 ppm in the carbimazole spectrum and shows no change in the spectrum of the complex.

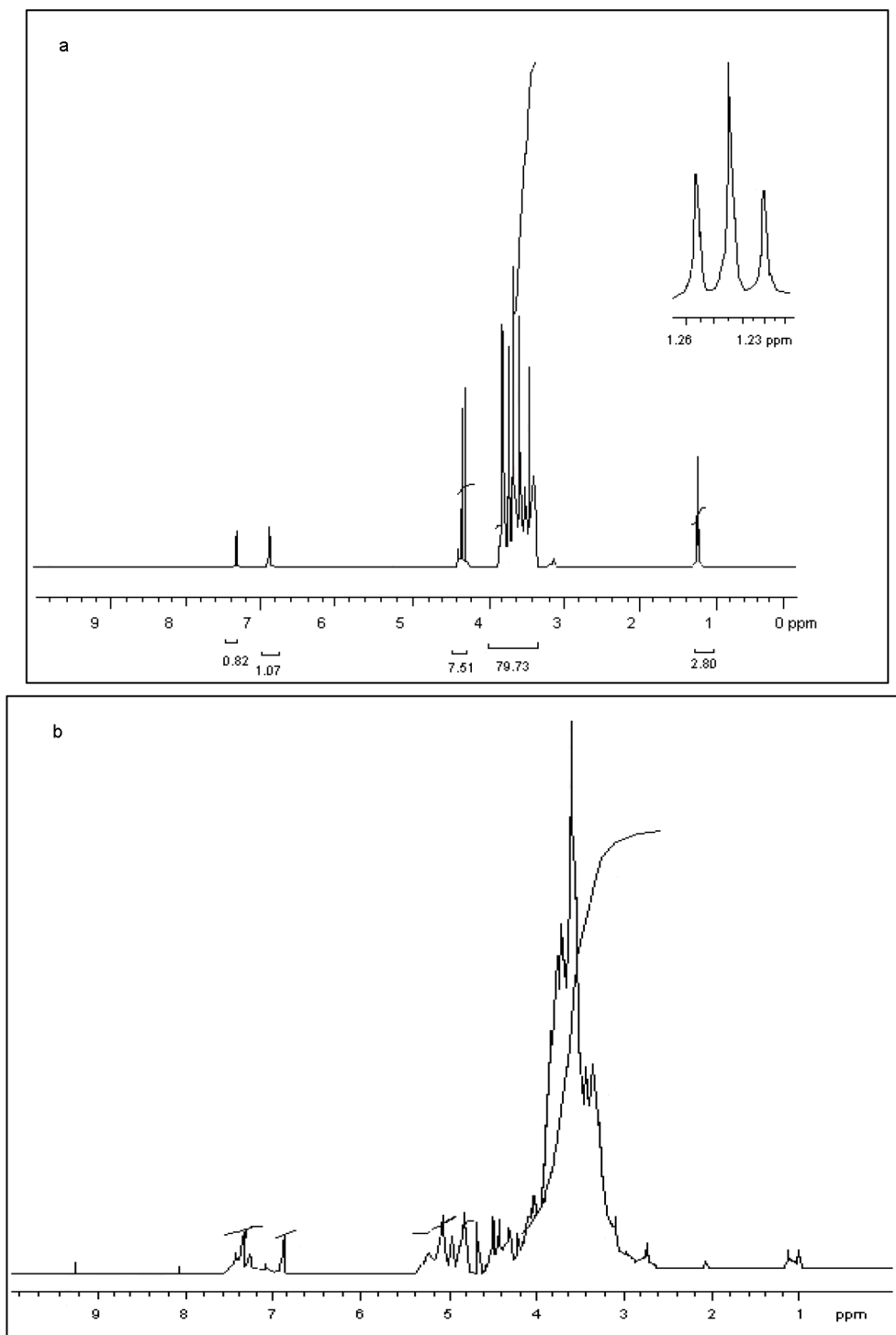


Figure 9. a, b) ^1H NMR spectrum of carbimazole and its Ru(III) complex.

A broadening of the peak observed in the region of 3–4 ppm accounts for the presence of an amino group. These amino groups have exchangeable H, capable of exchanging protons with the solvent D_2O to form DOH. Consequently, a crest arises at 4.2 ppm in the carbimazole:Ru(III) complex (Figure 9b). A peak of coordinated water can also be observed in the region of 3.5 ppm, as well as an aromatic N-CH_3 group, which also gives a

singlet peak in the region of 3.0–4.0 ppm. All these peaks get intermixed with one another and result in a broad band in the spectrum of the complex.

The FTIR and ^1H NMR data indicate that the binding of carbimazole with the Ru(III) ion takes place through sulfur and nitrogen functional groups.

2.5.3. ESR study

Scanning of the X-band in the electron spin resonance (ESR) spectrum of carbimazole (Figure 10a) revealed no resonance peak, thereby confirming its diamagnetic nature. The X-band for the carbimazole:Ru(III) complex (Figure 10b) gives an ESR signal at 1620 Gauss.

Calculation of Lande's G-factor (splitting factor):^{23,24}

$$g \text{ sample} = 20023 \left[1 - \frac{\Delta H}{H} \right]$$

where ΔH is the width between deflection points on the derivative absorption curve.

H =magnetic field

g_{Std} =Lande's factor for free electrons

$$g \text{ sample} = 20023 \left[1 - \frac{\Delta H}{H} \right]$$

$$g \text{ sample} = 20023 \left[1 - \frac{300}{1620} \right]$$

$$gq_{Std} = 1.631$$

The value of g obtained for the complex was quite low when compared to the g value of free electrons. This indicates the covalent nature of the complex owing to the d^5 electronic configuration.

2.5.4. Magnetic susceptibility measurement of the carbimazole:Ru(III) complex

The magnetic properties of the carbimazole:Ru(III) complex were determined using vibrating sample magnetometry (VSM). The magnetic moment (μ) value obtained was substituted into the following equation to calculate μ_{eff} .

$$X_m = \frac{\text{Molecular Weight} \times \text{slope} \times 1.1128 \times 10^{-21} \text{ B.M.}}{\text{Sample weight} \times 0.9273 \times 10^{-20}}$$

$$\text{where slope} = \frac{\mu(\text{magnetic moment in emu})}{H(\text{applied field in Gauss})}$$

$$\text{and } \mu_{eff} = 2.828\sqrt{X_m} \times \text{temperature}$$

The value of μ_{eff} was 1.65 BM, which is slightly lower than the expected value of 2.10 BM for a Ru(III) low spin complex. The decrease in the μ_{eff} value in the present case may be due to the lower symmetry ligand fields and electron delocalization. The value of μ_{eff} indicates that the number of unpaired electrons present in the central metal ion is equal to one. The hybridization state of the central metal ion Ru^{+3} has the valence

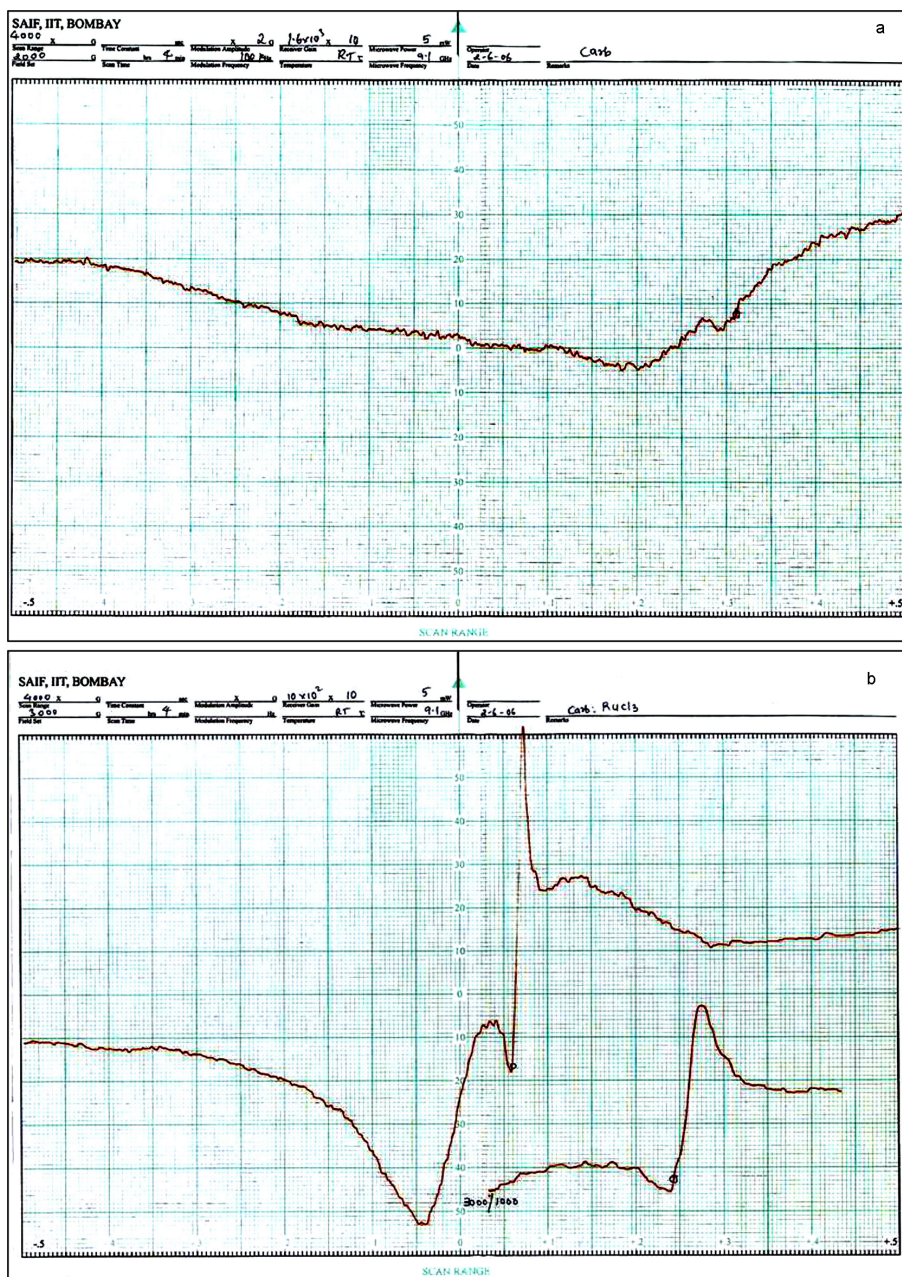


Figure 10. a, b) ESR spectra of carbimazole and its Ru(III) complex.

shell electronic configuration $4d^5 (t_{2g}^5, e_g^0)$, which is d^2sp^3 . Thus, ruthenium in its +3 oxidation state has a d^5 configuration and it forms low spin hexa-coordinated complexes with one unpaired spin. Thus, the carbimazole:Ru(III) complex is an inner orbital complex having octahedral geometry.

2.5.5. Thermogravimetric (TG) study

Both TG and DTG curves reveal a three-step decomposition process for the carbimazole:Ru(III) complex (Figure 11a) in the range of 34.15–800.8 °C. The first step shows a weak and small peak (T_{DTG} 100 °C) assigned to the slow decomposition of one lattice water molecule and one chlorine atom present outside the coordination

sphere, with weight loss of 0.77%. The second step, in contrast, is sharp and strong (T_{DTG} 223.54 °C) and accounts for the rapid removal of a coordinated water molecule attached to the Ru(III) ion, with a weight loss of 12.81%. The third step is small and weak (T_{DTG} 349.95 °C) and is assigned to the slow degradation of the drug moiety where C-C and C-H bonds begin to decompose, with a weight loss of 1.195%. Decomposition of the drug moiety continues up to 800 °C, leaving a final residue of elemental carbon and Ru(III). These results have also been confirmed by differential thermal analysis (DTA) (Table 3).

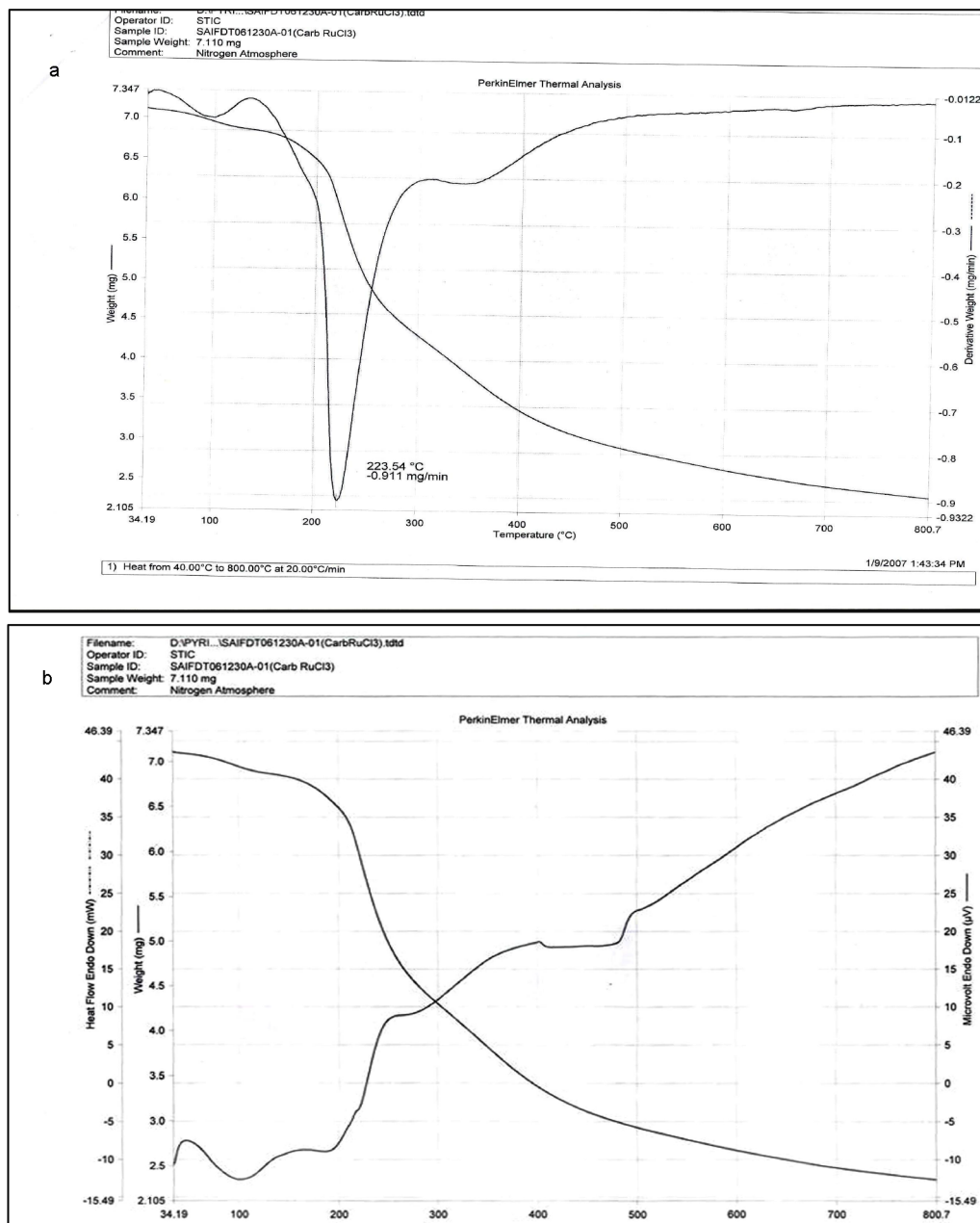


Figure 11. a, b) TG and DTA of the carbimazole:Ru(III) complex.

Table 3. Characteristic parameters of thermal decomposition.

Compound	Step	TG weight loss		$T_i / ^\circ\text{C}$	$T_f / ^\circ\text{C}$	$T_{DTG} / ^\circ\text{C}$
		Found (%)	Calculated (%)			
Carb:Ru(III)	1	0.79%	0.77%	66.70°	146.62°	100°
	2	12.83%	12.81%	200.0°	300.0°	223.54°
	3	1.196%	1.195%	300.0°	349.95°	419.8°

Carb = Carbimazole.

2.5.6. Differential thermal analysis

2.5.6.1. Endotherm at 100 °C

A moderate endothermic band (Figure 11b) starting at 66.70 °C and completing at 146.62 °C confirmed the loss of a coordinated water molecule. This was also suggested from the TGA curve.

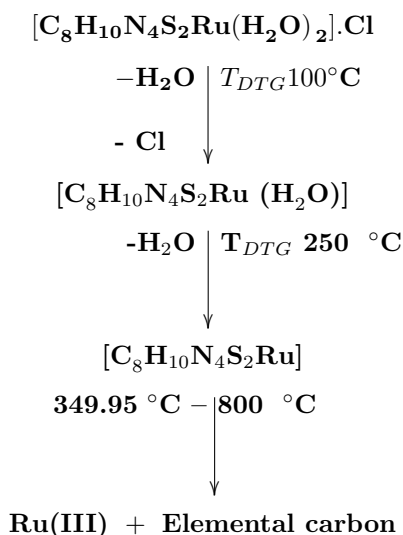
2.5.6.2. Exotherm from 200 °C to 300 °C

The exotherm band from 200 °C up to 300 °C is due to removal of coordinated water from the axial position. Here, a coordinated water molecule, when detached from the complex, decreases the Ru(III) metal ion. Consequently, Ru(III) is oxidized from its coordinated state.

2.5.6.3. Endotherm from 400 °C to 600 °C

A broad endotherm in the region from 400 °C to 600 °C was assigned to the breakdown of the drug moiety. These changes continue up to 800 °C, where the entire drug moiety is converted into its constituents, i.e. elemental carbon and residues of Ru(III).

The TGA and DTA results indicate the following decomposition steps:



2.5.7. Powder X-ray diffraction (PXRD) study

The powder X-ray diffractograms of Ru(III) (Figure 12a), carbimazole (Figure 12b), and its Ru(III) complex (Figure 12c) were obtained with the help of the Diffraction Plus basic evaluation package (EVA 10.0) of Bruker

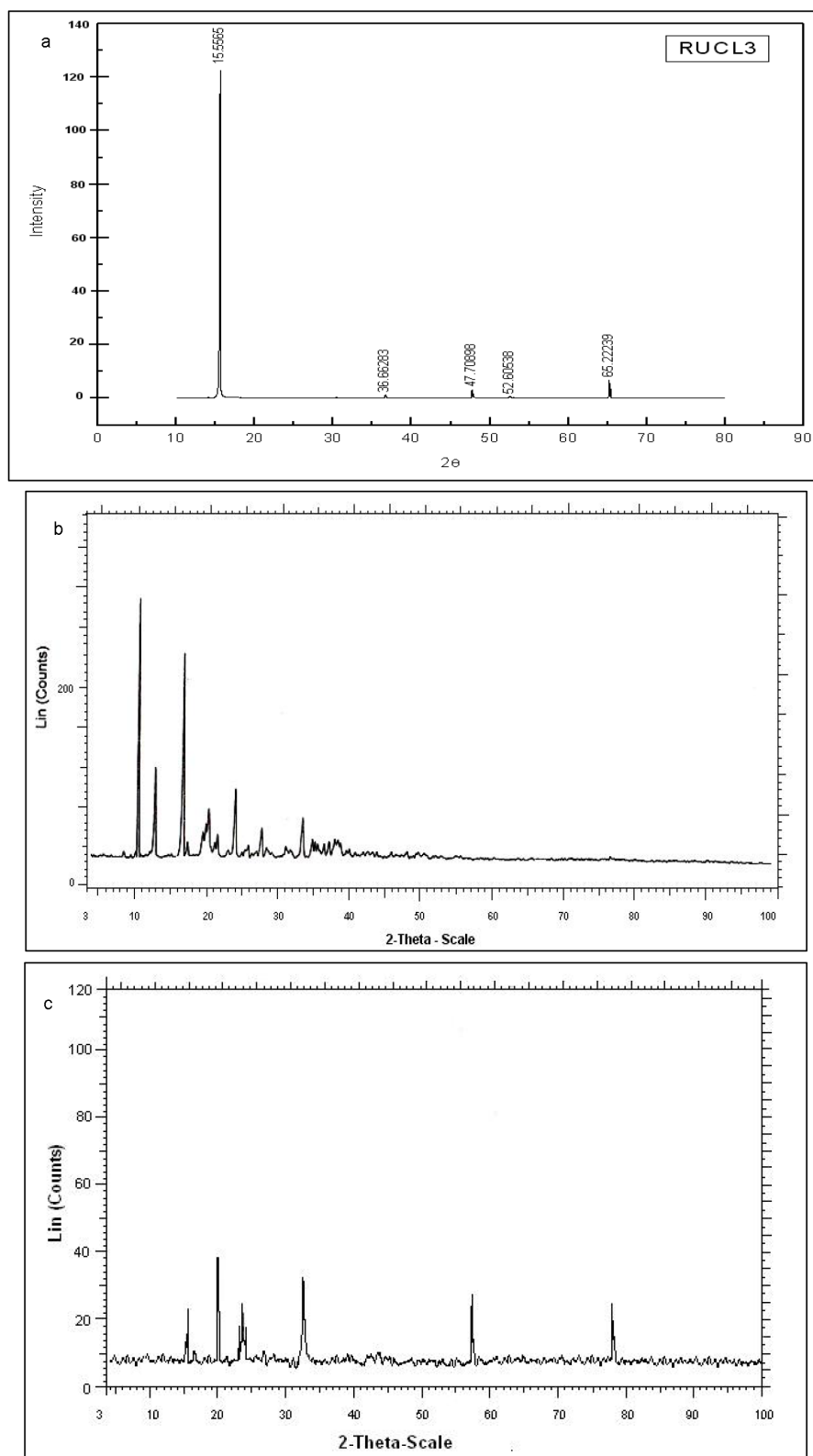


Figure 12. a, b, c) Diffractogram of Ru(III), carbimazole, and the carbimazole:Ru(III) complex.

Advanced X-ray Solutions. The data obtained using this software were further refined using Topaz software (version 10.0) to obtain lattice parameters, Miller indices, and crystallite size. Prediction of the diffractogram was done by matching the data with the JCPDS files (Joint Committee of Powder Diffraction Standards).

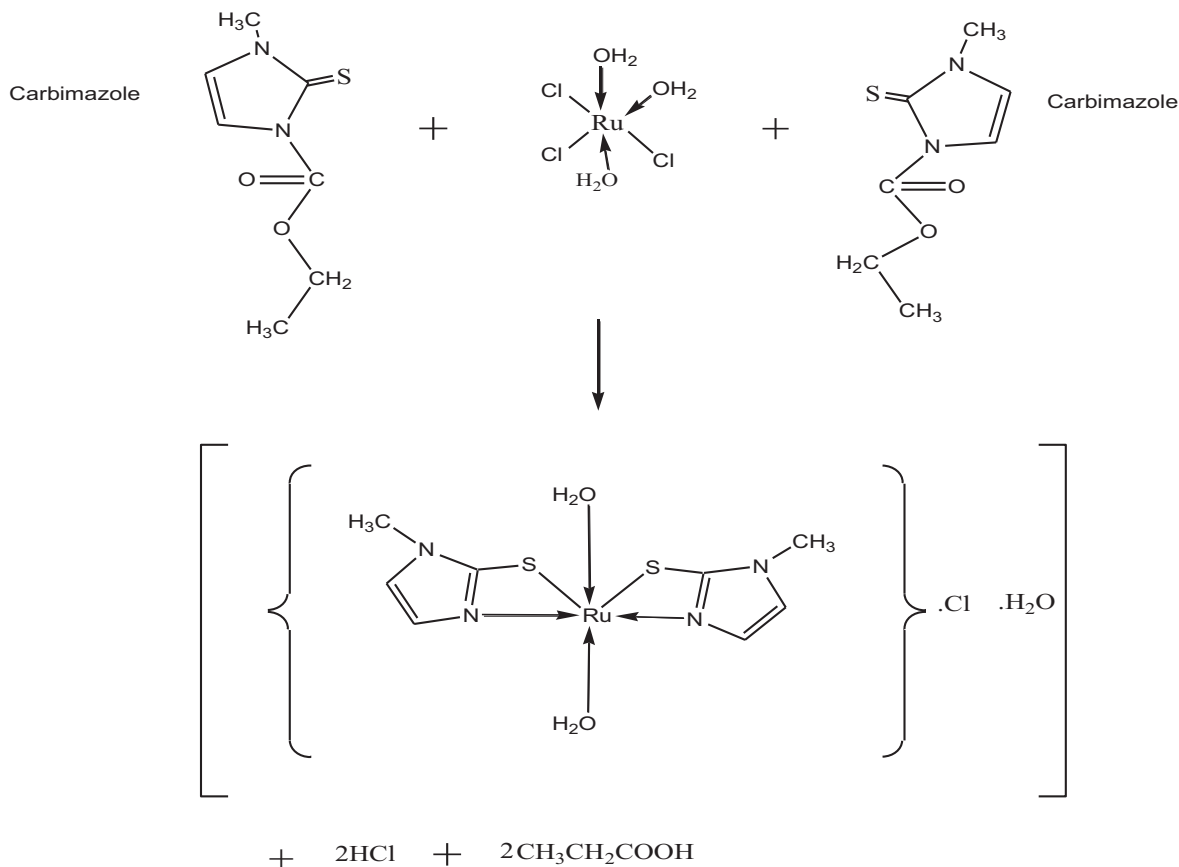


Figure 13. Proposed model for the carbimazole:Ru(III) complex.

The data obtained using the Topaz software shows that carbimazole has space group P2, R-Bragg 21.882, crystallite size 526.83 nm, and Miller indices (Table 4) with monoclinic crystal structure, whereas its complex has space group Pbma, R-Bragg 26.608, crystallite size 209 nm, and Miller indices (Table 4) with orthorhombic crystal structure, as confirmed by the following axial distance and axial angles:

Carbimazole	Carbimazole:Ru(III) complex
a (Å) = 12.075 $\alpha = 90^\circ$	a (Å) = 9.873 $\alpha = 90^\circ$
b (Å) = 11.082 $\beta = 117.762^\circ$	b (Å) = 14.642 $\beta = 90^\circ$
c (Å) = 15.750 $\gamma = 90^\circ$	c (Å) = 12.531 $\gamma = 90^\circ$

The powder X-ray diffractogram of carbimazole showed ten peaks with an angle range from 3° to 100°. Two high intensity peaks in the carbimazole diffractogram were assigned to:

$$(2\theta) 10.355^\circ, d = 8.535 \text{ \AA}, \text{Intensity} = 260, \text{Miller indices (hkl)} = 111$$

$$(2\theta) 16.603^\circ, d = 5.335 \text{ \AA}, \text{Intensity} = 210, \text{Miller indices (hkl)} = 121$$

Table 4. Powder X-ray diffraction data of carbimazole and its Ru(III) complex.

Carbimazole					Carbimazole: Ru (III) Complex				
S. no.	d-value	2θ	I	hkl	S. no.	d-value	2θ	I	hkl
1	8.535 Å°	10.355°	260	111	1	5.657	15.651	22.5	211
2	6.962 Å°	12.704°	95	002	2	4.323	20.523	38	102
3	5.335 Å°	16.603°	220	121	3	3.560	24.987	24	411
4	4.405 Å°	20.142°	55	201	4	3.329	32.846	33	342
5	4.146 Å°	21.415°	25	222	5	1.611	57.093	28	628
6	3.713 Å°	23.945°	71	311	6	1.218	78.452	24	4(10)5
7	3.451 Å°	25.795°	15	032					
8	3.220 Å°	27.673°	32	3(-2)(-3)					
9	2.683 Å°	33.366°	45	423					
10	2.419 Å°	37.137°	20	425					

whereas the remaining peaks were of medium and low intensity. These peaks were attributed to the presence of the thio group and were missing in the carbimazole:Ru(III) diffractogram. Furthermore, a comparison of the carbimazole diffractogram with the data reported in the literature indicated that carbimazole contains an imidazole moiety that strongly resembles the methyl benzimidazole moiety [PDF No. 3-1753].²⁵

The following are peaks found in common in both the carbimazole and benzimidazole motif:

$$(2\theta) 21.415^\circ, d = 4.1463 \text{ \AA}^\circ, \text{Intensity} = 25, \text{Miller indices (hkl)} = 222$$

$$(2\theta) 25.795^\circ, d = 3.4510 \text{ \AA}^\circ, \text{Intensity} = 15, \text{Miller indices (hkl)} = 032$$

$$(2\theta) 33.366^\circ, d = 2.6832 \text{ \AA}^\circ, \text{Intensity} = 45, \text{Miller indices (hkl)} = 423$$

These peaks were shifted in the diffractogram of carbimazole:Ru(III) as follows:

$$(2\theta) 24.987^\circ, d = 3.560 \text{ \AA}^\circ, \text{Intensity} = 24, \text{Miller indices} = 411$$

$$(2\theta) 32.846^\circ, d = 3.329 \text{ \AA}^\circ, \text{Intensity} = 7, \text{Miller indices} = 342$$

whereas the peak at (θ) 21.415° disappeared, suggesting the involvement of the imidazole ring of carbimazole in the complexation with the Ru(III) ion.

The peaks found in the diffractogram of carbimazole at

$$(2\theta) 12.704^\circ, d = 6.962 \text{ \AA}^\circ, \text{Intensity} = 95, \text{Miller indices (hkl)} = 002$$

$$(2\theta) 37.137^\circ, d = 2.419 \text{ \AA}^\circ, \text{Intensity} = 20, \text{Miller indices (hkl)} = 425$$

closely resembled those reported in the JCPDS File (PDF No. 37-0831), predicting the presence of an acetate group in the drug moiety. On complexation, this acetate group was detached from the parent moiety in acidic medium. Thus, these peaks were absent in the diffractogram of the complex.

Three new peaks were found in the diffractogram of the complex. These peaks were assigned to the binding of Ru(III) with sulfur and nitrogen atoms. This binding was also confirmed from the diffractogram data for pure trihydrated ruthenium trichloride (Figure 12a).

The PXRD data therefore suggest that carbimazole and its Ru(III) complex were crystalline in nature, with monoclinic and orthorhombic crystal structures.

Thus, these study results support the following proposed complexation model for carbimazole and Ru(III).

3. Experimental

UV-Visible spectra were recorded on a Unicam Helios spectrophotometer (Thermo, USA). FTIR spectra were recorded on a Shimadzu 8100 FTIR spectrometer (Japan) at the Department of Chemistry, Rani Durgavati University, Jabalpur, Madhya Pradesh, India.

^1H NMR spectra were obtained using a Varian 400 MHz spectrometer (USA) and D_2O CDCl_3 as the solvent, with tetramethylsilane (IIT Mumbai, India) as the internal standard. ESR spectra were recorded on a Varian spectrometer (USA) in the scan range of 2000 Gauss (G) at room temperature, using tetracyanoethylene as the marker (IIT Mumbai, India).

Thermogravimetric analysis (TG-DTA) was carried out at STIC Cochin University (Kerala, India) on a PerkinElmer thermal analysis system under nitrogen atmosphere in the 0–800 °C temperature range at a rate of 20 °C min^{-1} .

Powder XRD was performed on a Bruker Advance D8 Diffractometer (USA) at STIC Cochin University (Kerala, India). The diffractograms were scanned in the range of 0–100 with a maximum angular speed of 30° s^{-1} using Cu ($\lambda = 1.5406 \text{ \AA}$) as the X-ray source and a Si (Li) PSD detector.

3.1. Preparation of the ruthenium trichloride solution

A stock solution of ruthenium trichloride trihydrate ($\text{RuCl}_3 \cdot 3\text{H}_2\text{O}$) was prepared by dissolving an ampoule containing 1.0 g of Ru(III) (John Baker Inc., USA) in 250 mL of 2 M HCl in double distilled water to produce a volume of 1.0 L. The working solutions were made by dilution of this standard stock solution.

3.2. Preparation of carbimazole solution

Carbimazole tablets (brand name: Neomercazole) were obtained from Nicholas Piramal, Mumbai, India; each tablet contained 10 mg of carbimazole. One hundred milligrams of carbimazole was weighed and thoroughly mixed with 20 mL of distilled water, and the volume was made up to 100 mL by adding distilled water. The resulting mixture was filtered through No. 42 Whatman filter paper to avoid impurities. Standardization of the solution was done bromometrically.³ Solutions of lower concentration were made by dilution of the standard stock solution.

3.3. Procedure

To different aliquots (from 0.7 to 20 mL of a 5.76×10^{-4} M solution) of carbimazole were added equimolar amounts of Ru(III) solution (molarity 5.84×10^{-4} M). The solutions were allowed to stand for 20 min at room temperature. Absorbance was then recorded at the λ_{max} of the complex (370 nm) (Figure 2), which was found to differ from the λ_{max} of carbimazole.

Acknowledgment

The authors appreciate the assistance provided by the Sophisticated Analytical Instrumentation Facility (SAIF), IIT Powai Mumbai, IIT Roorkee, SAIF Punjab University, Chandigarh, and the Sophisticated Test Instrumentation Centre (STIC) Cochin University, Kerala, India, for the spectral analysis.

References

1. Furman, L. B. In *xPharm: The Comprehensive Pharmacology Reference*; Enna, S. J.; Bylund, D. B., Eds. Elsevier Science: Amsterdam, the Netherlands, 2007, pp. 1-4.
2. El Bardicy, M. G.; El-Saharty, Y. S.; Tawakkol, M. S. *Talanta* **1993**, *40*, 577-583.
3. Salah, M. S. *J. Pharmaceut. Biomed.* **1992**, *10*, 1059-1062.
4. Salah, M. S. *Anal. Sci.* **1992**, *8*, 503-504.
5. Ciesielski, W.; Zakrzewski, R.; Skowron, M. *Chem Anal.* **2001**, *46*, 873-881.
6. El Bardicy, M. G.; El-Saharty, Y. S.; Tawakkol, M. S. *Spect. Lett.* **1991**, *9*, 1079-1095.
7. Pedreno, S. C.; Albero, M. I.; Garcia, M. S.; Rodenas, V. *Anal. Chim. Acta* **1995**, *1-3*, 457-461.
8. Economou, A.; Tzanavaras, D. P.; Notou, M.; Themelis, G. D. *Anal. Chim. Acta* **2004**, *505*, 129-133.
9. El-Saharty, Y. S.; Abdel Kawy, M.; El Bardicy, M. G. *Spect. Lett.* **2001**, *34*, 325-334.
10. Zuman, P.; Fijalek, Z. *Anal. Lett.* **1990**, *23*, 1201-1212.
11. Zuman, P.; Fijalek, Z. *Anal. Lett.* **1990**, *23*, 1213-1233.
12. Deosarkar, A. V.; Deshpande, S. D.; Walode, S. G. *Der Phar. Sin.* **2012**, *3*, 388-393.
13. Ganasambandan, T.; Gunasekaran, S.; Seshadri, S. J. *Mol. Str.* **2013**, *1052*, 38-49.
14. Page, S. *Edu. Chem.* **2012**, *1*, 26-29.
15. Sharma, M.; Koty, A.; Al-Rajab, A. J. *Cur. Pharm. Anal.* **2017**, *13*, 999.
16. Ragehy, N. A.; Kawy, M. A.; Bayoumy, A. *Anal. Lett.* **1994**, *27*, 2127-2134.
17. Tirmizi, S. A.; Wattoo, F. H.; Wattoo, M. H. S.; Sarwar, S.; Memon, A. N.; Ghangro, A. B. *Arab. J. Chem.* **2012**, *5*, 309-314.
18. Coates, J. In *Encyclopedia of Analytical Chemistry*; Meyers, R. A., Ed. John Wiley: Chichester, UK, 2000, pp. 10815-10837.
19. Gnanasambandan, T.; Gunasekaran, S.; Seshadri, S. J. *Mol. Str.* **2013**, *1052*, 38-49.
20. Anacona, R. J.; Toledo, C. *Tran. Met. Chem.* **2001**, *26*, 228-231.
21. Vandersteen, O. S.; Vrublevska, T.; Lang, H. *Acta Chim. Slov.* **2004**, *51*, 95-106.
22. Nakamoto, K. N. *Infrared and Raman Spectra of Inorganic and Coordination Compounds*; Part V, 6th ed. Wiley and Sons: Chichester, UK, 1999.
23. Basosi, R.; Niccolai, N.; Rossi, C. *Bio. Chem.* **1978**, *8*, 61-69.
24. Wertz, E. J.; Bolton, R. J. *Electron Spin Resonance - Elementary Theory and Practical Applications*; 1st ed. McGraw-Hill: New York, NY, USA, 1972.
25. Das, D.; Roy, G.; Mugesh, G. *J. Med. Chem.* **2008**, *51*, 7313-7317.
26. Barzegar, M.; Rahmani, A.; Jabbari, A.; Mousavi, M. F. *J. Chinese Chem. Soc.* **2004**, *51*, 363-366.
27. Soledad, G. M.; Albero, M. I.; Sánchez, P. C.; Tobal, L. *Analyst* **1995**, *120*, 129-133.